Anonymous Referee #1

This study defines optimized Peak Over Threshold (POT) parameters and utilizing Longitudinal Wave Power (LWP) to identify significant morphological changes. The authors employed the Delft3D numerical model to simulate the morphological evolution of an idealized river mouth. This is an interesting work. However, there are some concerns regarding the absence of field validation, the significant simplification of model assumptions, and a potential over-reliance on specific parameters. Therefore, I recommend a Major Revision. Potentially useful suggestions are listed below:

The authors sincerely thank Reviewer 1 for their careful reading and insightful comments on our manuscript. In response to their suggestions, we have performed a sensitivity analysis as requested and revised and improved the manuscript accordingly.

Moreover, following the reviewers' suggestions, a new section has been incorporated into the manuscript to present the application of the methodology to two real-world study areas. These applications were carried out using previously calibrated and validated numerical models, whose calibration and validation were performed against real measured bathymetric data. This provides a meaningful empirical grounding for the methodology beyond the idealized framework, while also introducing real-world forcings including observed wave conditions, complete tidal regimes, and variable river discharges, and also different sediment grain sizes. As shown in the revised manuscript, the new Section 5, "Application to real-world study areas", reads as follows:

"*The methodology was applied to two different real-world study areas: the Punta Umbría Inlet, following Zarzuelo et al. (2019) and the Guadiana estuary, following López-Ruiz et al. (2020). For both study cases, models were implemented in Delft3D and have been calibrated and validated against field-measured bathymetric surveys, providing continuous morphological simulations over real observed periods. For the Punta Umbría Inlet, the model spans from July 2014 to October 2015, with model data obtained at 3-hour intervals. For the Guadiana estuary, two separate simulations with hourly data were utilized: (1) from July 2016 to June 2017, and (2) from June 2017 to December 2018. This section presents the match results for each simulation using the two primary POT combinations: T-POT and Combination 11.*

5.1. Punta Umbría Inlet

The Punta Umbría Inlet (hereinafter PUI) consists of a NW-SE trending channel, 8 km in length and 0.5 km in width, with a maximum depth of -12 m MSL. Characterized as an ebb-tidal system, it features minor ebb channels, shoals, and frontal lobes. The model utilizes a spatially distributed D_{50} sediment grain size, ranging from 0.5 to 4 mm. This is defined via a grid-based input file to reflect the natural variability of the seabed. Due to long-standing navigational difficulties associated with shoal development, a jetty was constructed at the inlet, reaching -4 m MSL. The numerical setup and validation procedures follow Zarzuelo et al. (2019) in their entirety. A comprehensive description of the model performance is available in that study.

The control volume used to apply the methodology is located in the channel (Figure S11 from Supplementary Material). The match values obtained for the T-POT are 43.4% and 41.4% for the LWP-ME90 and LWP-ME95, respectively, and 42,7% and 45,1% for the H_s-ME90 and H_s-ME95,

respectively. For the optimal combination (Combination 11, POT(95,4,6)), the match results for LWP increase to 47.4% (ME90) and 47.5% (ME95), while the H_s matches remain identical to those of the T-POT. This suggests that the optimal POT combination improves upon the T-POT for LWP while maintaining the same accuracy for H_s.

5.2. Guadiana estuary

The numerical setup for the Guadiana estuary follows the configuration described in López-Ruiz et al. (2020), where a comprehensive description of the model's calibration and performance is available. The study area encompasses the ebb-tidal delta of the Guadiana River, located at the southern border between Spain and Portugal. The region is characterized by a semi-diurnal mesotidal regime, with a mean tidal range of 2 m. Similar to the PUI, the river mouth is stabilized by a jetty system, and the main channel undergoes periodic dredging to maintain navigability. Sediment distribution in the area exhibits the high variability typical of deltaic environments, with grain sizes ranging from fine to coarse sands. The model utilizes a spatially distributed D_{50} sediment grain size, ranging from 1 to 10 mm. This is defined via a grid-based input file to reflect the natural variability of the seabed.

Two simulations covering different periods are available for this study area, hereafter referred to as Guadiana 1617 (from July 2016 to June 2017) and Guadiana 1718 (from June 2017 to December 2018). The control volume used to apply the methodology is located in the ebb delta, within an area comparable to the one analyzed by Garel et al. (2019) to unravel the sediment transport patterns in the delta (Figure S12 from Supplementary Material).

For Guadiana 1617, the match values obtained for the T-POT are 63.5% and 62.9% for the LWP-ME90 and LWP-ME95, respectively, and 64.3% and 63.9% for the H_s-ME90 and H_s-ME95, respectively. For the optimal combination (Combination 11, POT(95,4,6)), the match results for LWP increase to 67.5% (ME90) and 67.9% (ME95), while the H_s matches remain identical to those of the T-POT.

For the Guadiana 1718 period, the T-POT achieved match values of 72.3% and 90.5% for LWP (ME90 and ME95, respectively), and 73.1% and 90.5% for H_s. The optimal POT combination (Combination 11) improved the LWP-ME90 match to 79% and the H_s-ME90 to 74.4%, while maintaining identical results for all ME95 events. Notably, almost all ME95 morphological events occurred during Storm Emma (February 2018), which heavily impacted the South Atlantic coast of the Iberian Peninsula (Málvarez et al. 2021)."

As demonstrated, the application to real-world scenarios confirms the robustness of the methodology. The optimal POT combination (Combination 11) consistently outperforms the T-POT across the three simulations analyzed regarding LWP matches. The single exception is the Guadiana 1718 case, where the dominance of a single extreme event (Storm Emma) concentrates nearly all ME95 events within a brief period, thereby limiting the discriminatory capacity of the LWP-based proxy under such specific conditions. This behavior is consistent with the role of the LvC index discussed in Section 6.1 of the revised manuscript (and further detailed in our response to Comment 1), reinforcing the complementary nature of LWP and Hs as morphological proxies. Moreover, the Hs related matches for the optimal POT combination are equal to the T-POT matches, with the exception of Guadiana 1718, where the match for Hs-ME90 shows an improvement over the T-POT.

Storm Emma (February 28 – March 5, 2018) was a severe Atlantic event that triggered extreme meteorological and oceanographic conditions across the southwestern Iberian Peninsula. It produced a 22-year record significant wave height of 7.27 m and raised sea levels to 4.12 m through a combination of low atmospheric pressure and spring tides. These forces caused profound morphodynamic changes, including dune erosion of 2.5 m and the modification of seabed elevation at depths as great as -10 m (García-de-Lomas, et al., 2019; Málvarez et al. 2021).

The Figures S11 and S12 from the Supplementary Material correspond to Figure 1 and Figure 2, respectively, from the present document.

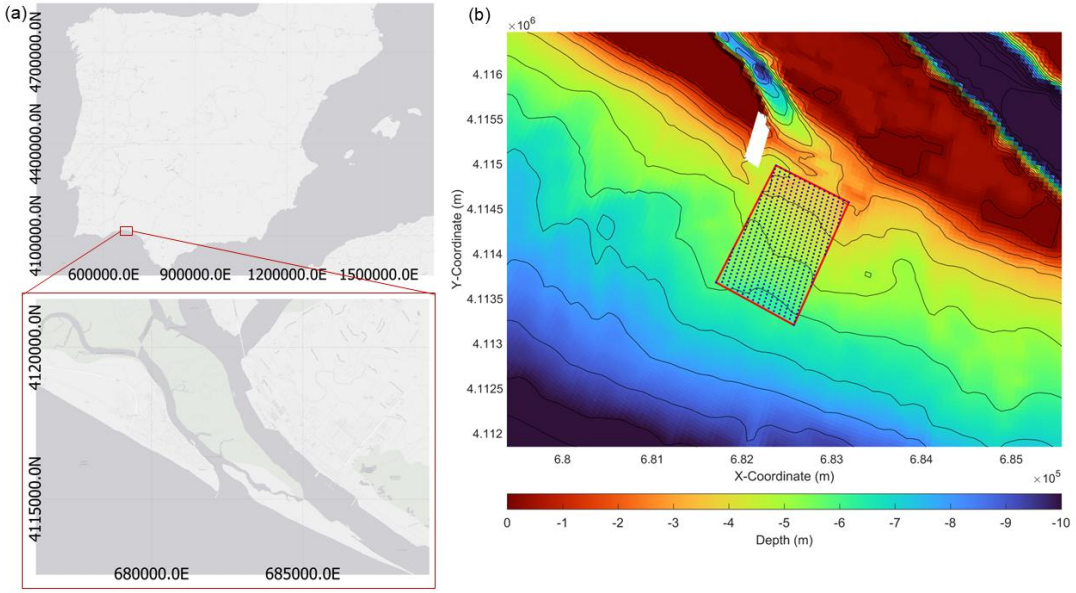

Figure 1. (a) Study area location in the Iberian Peninsula. (b) Control volume for the Punta Umbría Inlet shown on the actual bathymetry of the area. Bathymetric contours are represented every 1m, from 0 to -12 m MSL.

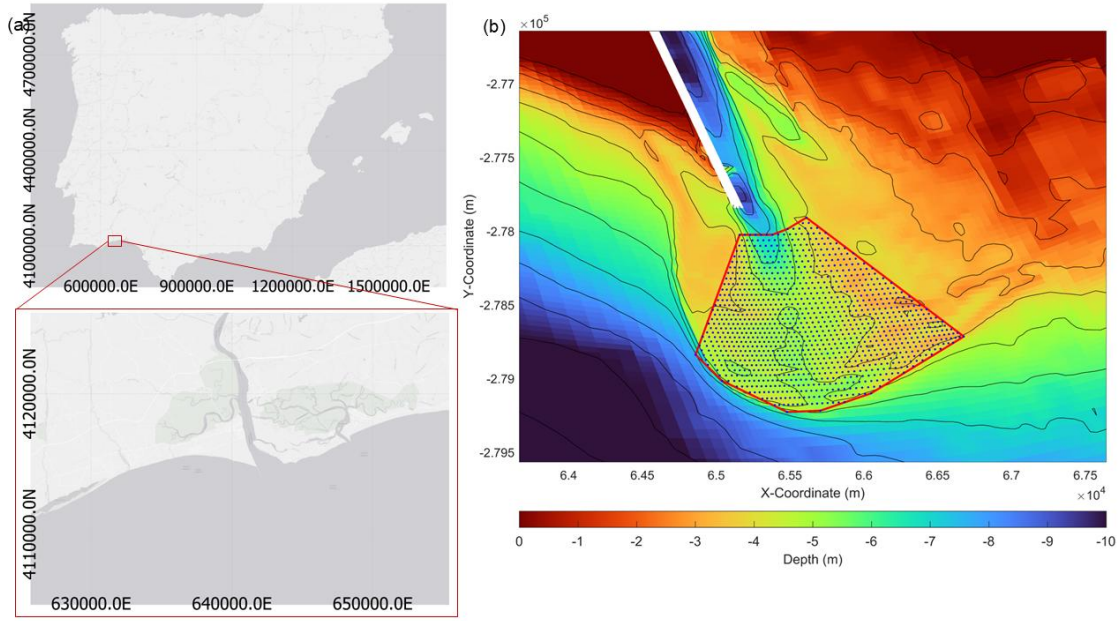

Figure 2. (a) Study area location in the Iberian Peninsula. (b) Control volume for the Guadiana Estuary shown on the actual bathymetry of the area. Bathymetric contours are represented every 1 m, from 0 to -12 m MSL.

1. **While the authors have cited extensive literature on storm erosion, there appears to be limited discussion on existing studies that also utilize Wave Power or Energy Flux for prediction purposes. Expanding this section would strengthen the context.**

Following the reviewer's recommendation, the Introduction and Section 6.1 (formerly Section 5.1) have been updated to include additional references on the use of Wave Energy Flux and Wave Power in coastal risk assessment, and to demonstrate how they align with the methodology proposed in this study.

Recent literature has increasingly adopted Wave Energy Flux (WEF) and Wave Power as fundamental metrics in coastal risk evaluation. Mentaschi et al. (2017) utilize the 100-year return level of WEF as a robust proxy for both coastal flooding and erosion. This approach is supported by the work of Pinson et al. (2012), who emphasize that because WEF represents the actual power available in the sea, it is the central variable for understanding the physical stress applied to the coastal environment. More recently, Rusu (2022) demonstrated that the spatial distribution of wave power is heavily influenced by local bathymetry, highlighting its relevance for site-specific coastal planning.

In line with this body of literature, a relationship between wave energy and sediment transport can be further quantified to distinguish the specific nature of coastal changes. López-Dóriga and Ferreira (2017) proposed the Longshore vs. Cross-shore (LvC) index, which relates wave energy conditions to volumetric sediment changes to determine whether a storm event or coastal area is longshore-dominated or cross-shore-dominated. This index has been incorporated into the present study in section 6.1 "The role of wave direction" (formerly Section 5.1) of the revised manuscript, reading as follows: "*Furthermore, by applying the LvC (Longshore vs. Cross-shore) index proposed by López-Dóriga and Ferreira (2017), it was found that the NCV exhibits a more cross-shore dominated in experiment 2 (1990-91) with an LvC=0.18, and in experiment 5 (2010-11) with LvC=0.01, both of which correspond to a higher H_s-match. Conversely, the SCV shows systematically higher LvC across most experiment, indicating a greater degree of longshore dominance, which corresponds with a higher LWP-match. The calculated LvC indices for all experiments and control volumes are provided in Table S5 of the Supplementary Material.*".

Table S5 from the Supplementary Material corresponds to Table 1 of the present document.

Table 1. LvC index calculated for each CV and for each experiment.

Year (Experiment)	NCV	SCV
1980-1981 (1)	0.25	0.30
1990-1991 (2)	0.18	0.60
1999-2000 (3)	0.85	0.66
2000-2001 (4)	0.38	0.44
2010-2011 (5)	0.01	0.40
2019-2020 (6)	0.17	0.75

Additionally, the text added in the Introduction reads as follows: *"Furthermore, some studies have employed the Wave Energy Flux or the Wave Power for coastal risk evaluation. For instance, in Mentaschi et al. (2017), where they use the 100-year return level of Wave Energy Flux as a robust*

proxy for both coastal flooding and erosion. More recently, Rusu (2022) demonstrated that the spatial distribution of wave power is heavily influenced by local bathymetry, highlighting its relevance for site-specific coastal planning"

2. **It is recommended that the authors also highlight the deficiencies of existing statistical methods, rather than solely focusing on the neglect of physical processes.**

We thank the reviewer for this suggestion. The POT methodology was originally developed to improve upon the Annual Maxima Method (AMM), which assumes that annual maximum values are independent and identically distributed. A significant limitation of the AMM is its reliance on a single value per year, whereas the POT method allows for the inclusion of multiple extreme events (Mendez et al. 2006). Therefore, the POT model utilizes a sample of major storms considerably larger than the number of annual maxima.

However, the deficiencies of the POT method primarily relate to parameter selection. As noted by Almarshed (2025), the selection of an appropriate threshold must balance two competing requirements: it must be high enough to ensure the statistical independence of events, yet not so restrictive as to exclude a significant number of relevant extremes. This trade-off is inherently context-specific, as POT parameters vary across different geographic regions and wave climate conditions.

The POT methodology is widely used. However, the importance of site-specific parameters is a key consideration already addressed in the manuscript. As stated in the manuscript (Section 3): *"Even though coastal storm thresholds are site-specific (Harley, 2017), the existing literature lacks a unified criterion for these parameters even within the same geographical regions. Storm definitions are commonly different between authors, and storm thresholds are often selected arbitrarily, with the statistical and meteorological independence between storm events frequently being neglected (Kummerer et al., 2024). This non-uniformity is evident in the threshold selection: for instance, studies on the Mediterranean Sea utilize varying wave height thresholds, such as the 95th percentile (Martzikos et al., 2021), 96th percentile (Del-Rosal-Salido et al., 2025), or 98th percentile (Sanuy et al., 2024).*

Similarly, the minimum storm duration exhibits significant regional variability: it ranges from 6 hours (Mendoza et al., 2011) to 12 hours (Ojeda et al., 2017) for the Mediterranean Sea, while on the Atlantic coast (Portugal and West Andalusia), the range is even wider, varying from 12 hours (Puig et al., 2016) to 48 hours (Almeida et al., 2012). Regarding the independence criterion, which is typically approached using a fixed value (Martzikos et al., 2021), the values shown in Table 2 were selected to cover the observed range in literature. This range extends from the lower boundary of 30 hours, established for the South Portuguese coast (Almeida et al., 2012), to the upper limit of 96 hours (Martzikos et al., 2021). However, since the POT combinations analyzed included a minimum storm duration of 48 hours, adopting an independence interval shorter than this would lack physical consistency. Consequently, the lower boundary was fixed at 48 hours (2 days)."

3. **Since these parameters are inherently site-specific, a systematic evaluation of 45 POT parameter combinations was carried out in this study to identify the configuration that best captures morphologically significant events at the study site. Lines 119-120; Table 1: Table 1 shows that the mean significant wave height (Hs) for six selected years is very similar (1.00m - 1.11m). Does this limit the testing of the method under extremely variable climates?**

We acknowledge the reviewer's observation. While the mean Hs values are indeed similar across the six selected years — as they correspond to the same geographic location and therefore share a common regional wave climate — the percentile distribution and energy characteristics vary considerably between years. The primary objective of this study was to evaluate the method's sensitivity to inter-annual variability in energy distribution at a specific site, rather than to compare fundamentally different wave climates. Focusing on a single representative location allowed for a high-resolution assessment of event-based changes while maintaining a manageable computational cost and minimizes confounding factors associated with differences in regional oceanographic settings. We have clarified this in Section 2.2. "Hydrodynamic Forcings" of the revised manuscript, which now reads as follows: *"While mean H_s values were similar (1.00–1. 11 m), the most extreme waves (e.g. H_s 99th) showed greater variability, ranging from 2,89 m to 3,76 m (Table 1). This selection focuses on a single representative site to evaluate the methodology's sensitivity to inter-annual variability in wave energy distribution, rather than climatic shifts across different locations. This approach ensures consistency in regional characteristics while maintaining a manageable computational cost for high-resolution event-based analysis".*

4. **Lines 135-136; Line 576: A constant river discharge of 10 m^3/s is used in the model setup. However, in reality, storm events causing significant wave height changes often coincide with heavy rainfall and high river discharge. Neglecting the surge in discharge during storms might lead to a misinterpretation of the storm events and their driving mechanisms.**

The authors acknowledge the referees' concerns regarding the simplified initial conditions. The use of a constant river discharge in the idealized simulations was a deliberate methodological choice, consistent with established idealized modeling frameworks in coastal morphodynamics (e.g., Jiménez-Robles et al., 2016; Ruiz-Reina & López-Ruiz, 2021). In this context, the constant discharge allows us to isolate the morphological response driven specifically by wave-induced processes, minimizing the confounding influence of fluvial forcing on the results.

However, we believe that the application of the methodology to real-world scenarios, as discussed in the previous response and in the revised manuscript, addresses these concerns. In those cases, the bathymetries reflect natural sediment variability (including spatially distributed D_{50}), and the forcing inputs are based on empirical data, including complete tidal regimes, variable river discharges, and explicit wind forcing alongside buoy-derived wave data. Furthermore, the concurrent increase in river discharge during storm events is a physically relevant process (particularly in fluvially influenced systems such as the Guadiana estuary and the Punta Umbría Inlet) which is now explicitly accounted for in our real-world validation.

The results demonstrate that the methodology remains robust even when these additional environmental complexities are introduced. Since the effectiveness of the approach is captured in both controlled idealized cases and complex natural environments, we believe the current scope provides a comprehensive validation of its robustness.

To further clarify this point (and the related to the previous comment), we have added a discussion of these considerations in Section 6.3 (formerly Section 5.3) “Limitations and further improvements” , which now reads: *“Although the method was developed following established idealized frameworks (e.g., Jiménez-Robles et al., 2016; Ruiz-Reina & López-Ruiz, 2021), its successful validation in calibrated environments with real-world forcings, which include wind, variable river discharge, and full tidal regimes, addresses the applicability to complex coastal zones and supports the robustness of the methodology under more complex forcing conditions.”*

5. **Lines 210-213; Lines 588-590: This study is entirely based on an idealized numerical model. Although the authors acknowledge the lack of field data comparison in Section 5.3, without empirical data validation, the so-called "optimal POT parameter combination" (95th percentile, 4-day independence, etc.) might merely be an artifact of the specific model settings. It is suggested that the authors at least discuss the robustness of these optimal parameters if model settings (such as friction coefficients or diffusion coefficients) were to change.**

Following the reviewers’ recommendation, eight new simulations were conducted as a sensitivity analysis. Maintaining all other parameters constant, the uniform horizontal eddy viscosity (originally set to 2 m^2/s) was tested at values of 1 and 5 m^2/s. Additionally, two Chèzy roughness coefficients (60 and 70) were evaluated against the original value of 65. These four sensitivity scenarios were performed for two different experiments from the original study: (1) 1980–1981 and (3) 1999–2000.

After applying the methodology proposed in the paper, the matches obtained for the Traditional POT combination (T-POT, POT(95, 3, 12)) and the Optimal POT combination POT(95, 4, 6) were compared (Table 2). The results yielded identical match percentages in all cases, demonstrating the robustness of the model and the stability of the optimal parameters.

This information has been added to the Section 2.4 “Model setup and experimental design” in the revised manuscript, and the corresponding table has been included in the Supplementary Material (Table S4, Table 2 from the present document). The text included reads as follows: “*A sensitivity analysis was conducted through eight additional simulations to assess the robustness of the methodology with respect to key model parameters. While maintaining all other parameters constant, the uniform horizontal eddy viscosity was tested at values of 1 and 5 m^2/s, and two Chèzy roughness coefficients (60 and 70, in both directions) were evaluated for comparison with the original values. These four sensitivity scenarios were performed for two representative experiments (1980–1981 and 1999–2000). The match percentages obtained for both the T-POT and the optimal POT combination were identical across all sensitivity scenarios (Table S4), confirming that the identified optimal parameter combination is independent of these numerical settings.*”

Table 2. Match results obtained for the T-POT (POT(95,3,12)) and the Optimal POT combination (POT(95,4,6)), including the original simulation and sensitivity analyses of uniform horizontal eddy viscosity (ε) and Chèzy roughness coefficients.

			LWP-ME90		Hs-ME90		LWP-ME95		Hs-ME95	
			NCV	SCV	NCV	SCV	NCV	SCV	NCV	SCV
1980-1981	T-POT	**Original**	**49.4**	**55.8**	**34.1**	**32**	**65.5**	**82.5**	**53.4**	**55.6**
		ε=1	49.4	55.8	34.1	32	65.5	82.5	53.4	55.6
		ε=5	49.4	55.8	34.1	32	65.5	82.5	53.4	55.6
		Chèzy=60	49.4	55.8	34.1	32	65.5	82.5	53.4	55.6
		Chèzy=70	49.4	55.8	34.1	32	65.5	82.5	53.4	55.6
	Optimal POT combination	**Original**	**53.2**	**55.8**	**37.1**	**35.5**	**72.9**	**82.9**	**53.4**	**62.6**
		ε=1	53.2	55.8	37.1	35.5	72.9	82.5	53.4	62.6
		ε=5	53.2	55.8	37.1	35.5	72.9	82.5	53.4	62.6
		Chèzy=60	53.2	55.8	37.1	35.5	72.9	82.5	53.4	62.6
		Chèzy=70	53.2	55.8	37.1	35.5	72.9	82.5	53.4	62.6
1999-2000	T-POT	**Original**	**50.2**	**53.3**	**36.2**	**35**	**63**	**68.25**	**47**	**36.1**
		ε=1	50.2	53.3	36.2	35	63	68.25	47	36.1
		ε=5	50.2	53.3	36.2	35	63	68.25	47	36.1
		Chèzy=60	50.2	53.3	36.2	35	63	68.25	47	36.1
		Chèzy=70	50.2	53.3	36.2	35	63	68.25	47	36.1
	Optimal POT combination	**Original**	**53.5**	**56.7**	**51.1**	**48.1**	**66.5**	**72.4**	**63.3**	**56.4**
		ε=1	53.5	56.7	51.1	48.1	66.5	72.4	63.3	56.4
		ε=5	53.5	56.7	51.1	48.1	66.5	72.4	63.3	56.4
		Chèzy=60	53.5	56.7	51.1	48.1	66.5	72.4	63.3	56.4
		Chèzy=70	53.5	56.7	51.1	48.1	66.5	72.4	63.3	56.4

6. **Table 2; Lines 253-255: The independence criterion in Table 2 tests intervals of 2, 3, and 4 days. However, for certain storm clusters, the interval might be less than 2 days. Why were shorter intervals (e.g., 24 or 36 hours) not tested?**

The choice of the independence criterion from 2 days to 4 days is well-supported by the literature in different oceanic regions. According to Mathiesen et al. (1994), an interval of 2 to 4 days is generally sufficient to guarantee the independence of extreme events. This is consistent with Méndez et al. (2006), who identified 3 days as the optimal threshold for independence, and Luceño et al. (2006), who noted that while statistical fit may improve with 3 to 6 days, they also pointed out that longer intervals risk a significant loss of data. More recent studies, such as Almarshed (2025), also report that intervals between 1 and 4 days are common practice in POT analyses of extreme wave heights. This range was selected to maintain a balance between ensuring physical independence and preserving a robust sample size. Furthermore, since the POT combinations studied included a minimum storm duration of 48 hours, adopting an independence interval shorter than this would lack physical consistency.

7. **Lines 320-324: The method defines a "match" if the wave height is observed within 24 hours after a climatic event. This 24-hour time lag seems to lack a strong physical or statistical basis. The authors should provide a sensitivity analysis or cite relevant literature to support this specific timeframe.**

The authors understand the reviewer's concern regarding this decision. To justify the 24-hour time lag, a preliminary sensitivity test was conducted evaluating different intervals: no lag, 3, 12, 24, and 48 hours. The 24-hour window was selected as provided the best synchronization between climatic events and the morphological events, as evidenced by the alignment of event occurrences (e.g., the correspondence between 'red dots' and 'black dots' in Figures 4 and 5).

While the authors acknowledge the importance of sensitivity analyses, they believe that including the full results of this test would unnecessarily increase the length and complexity of the manuscript, which is already quite extensive. Nevertheless, the consistency of this timeframe is further supported by the results shown across the Supplementary Material (Figures S1–S10), where the 24-hour lag yields physically realistic and consistent morphological interpretations across all simulated years. This interval is also physically consistent with the morphodynamic response timescale of mesotidal wave-dominated systems, where significant net volumetric changes typically develop over periods of hours to tens of hours following the onset of energetic forcing conditions.

8. **Lines 420-425: The results show that in some cases, LWP misses certain events. In the Discussion section, it would be more balanced to point out that LWP serves as a complementary proxy to Hs for capturing directional events, rather than implying it can completely replace Hs. The current phrasing occasionally appears too dismissive of Hs.**

We thank the reviewer for this constructive observation. We agree that the manuscript should present LWP as a complementary proxy to Hs rather than as a complete substitute, and we have revised the text accordingly. We have added the following sentences to discussion Section 6.2 (formerly Section 5.2), "Main novelties and methodological advances"**:** "*It should be noted, however, that the superior performance of LWP does not preclude the utility of Hs as a morphological proxy. In coastal settings characterized by a low LvC index, where cross-shore processes dominate sediment transport, H_s remains a more accurate indicator of morphologically significant events, suggesting that LWP serves as a complementary proxy rather than a total replacement.*"

References used

Almarshed, B. F.: Optimizing threshold selection for accurate prediction of long-term extreme wave heights, Journal of Engineering Research (Kuwait), 13, 2965–2983, https://doi.org/10.1016/j.jer.2024.12.005, 2025.

García-de-Lomas, J., Payo, A., Cuesta, J. A., and Macías, D.: Morphodynamic study of a 2018 mass-stranding event at Punta Umbria Beach (Spain): Effect of Atlantic Storm Emma on Benthic Marine Organisms, J Mar Sci Eng, 7, https://doi.org/10.3390/jmse7100344, 2019.

Jiménez-Robles, A. M., Ortega-Sánchez, M., and Losada, M. A.: Effects of basin bottom slope on jet hydrodynamics and river mouth bar formation, J Geophys Res Earth Surf, 121, 1110–1133, https://doi.org/10.1002/2016JF003871, 2016.

López-Dóriga, U. and Ferreira, Ó.: Longshore and cross-shore morphological variability of a berm-bar system under low to moderate wave energy, J Coast Res, 33, 1161–1171, https://doi.org/10.2112/JCOASTRES-D-16-00050.1, 2017.

Luceño, A., Menéndez, M., and Méndez, F. J.: The effect of temporal dependence on the estimation of the frequency of extreme ocean climate events, Proceedings of the Royal Society A: Mathematical, Physical and Engineering Sciences, 462, 1683–1697, https://doi.org/10.1098/rspa.2005.1652, 2006.

Málvarez, G., Ferreira, O., Navas, F., Cooper, J. A. G., Gracia-Prieto, F. J., and Talavera, L.: Storm impacts on a coupled human-natural coastal system: Resilience of developed coasts, Sci. Total Environ., 768, 144987, https://doi.org/10.1016/j.scitotenv.2021.144987, 2021.

Mathiesen, M., Goda, Y., Hawkes, P. J., Mansard, E., Martín, M. J., Peltier, E., Thompson, E. F., and van Vledder, G.: Methodes conseillées pour 1'analyse des houles extreme, Journal of Hydraulic Research, 32, 803–814, https://doi.org/10.1080/00221689409498691, 1994.

Méndez, F. J., Menéndez, M., Luceño, A., and Losada, I. J.: Estimation of the long-term variability of extreme significant wave height using a time-dependent Peak Over Threshold (POT) model, J Geophys Res Oceans, 111, https://doi.org/10.1029/2005JC003344, 2006.

Mentaschi, L., Vousdoukas, M. I., Voukouvalas, E., Dosio, A., and Feyen, L.: Global changes of extreme coastal wave energy fluxes triggered by intensified teleconnection patterns, Geophys Res Lett, 44, 2416–2426, https://doi.org/10.1002/2016GL072488, 2017.

Pinson, P., Reikard, G., and Bidlot, J. R.: Probabilistic forecasting of the wave energy flux, Appl Energy, 93, 364–370, https://doi.org/10.1016/j.apenergy.2011.12.040, 2012.

Ruiz-Reina, A. and López-Ruiz, A.: Short-term river mouth bar development during extreme river discharge events: The role of the phase difference between the peak discharge and the tidal level, Coastal Engineering, 170, 103982, https://doi.org/10.1016/j.coastaleng.2021.103982, 2021.

Rusu, L.: The near future expected wave power in the coastal environment of the Iberian Peninsula, Renew Energy, 195, 657–669, https://doi.org/10.1016/j.renene.2022.06.047, 2022